THE JOURNAL OF PHYSICAL CHEMISTRY Letters

PERSPECTIVE

pubs.acs.org/JPCL

Light Concentration at the Nanometer Scale

Ramón Alvarez-Puebla,[†] Luis M. Liz-Marzán,*[,†] and F. Javier García de Abajo*[,‡]

[†]Departamento de Química Física and Unidad Asociada CSIC-Universidade de Vigo, 36310 Vigo, Spain, and [‡]Instituto de Óptica, CSIC and Unidad Asociada CSIC-Universidade de Vigo, Serrano 121, 28006 Madrid, Spain

ABSTRACT Visible and near-infrared optical excitations are common currency in the biological world, and consequently, they are routinely used to investigate microscopic phenomena taking place in living organisms and their environment. However, the wavelength of light within that energy region is above hundreds of nanometers, thus averting the possibility of direct nanometer-scale resolution. We show in this Perspective that narrow gaps between metals and sharp tips in colloidal gold particles constitute excellent "light confiners" that permit solving this problem, and in particular, they lead to record levels of surface-enhanced Raman scattering. Our results are framed in the context of a historical quest toward achieving optical focusing in the near field, and we offer a tutorial explanation of why evanescent waves such as plasmons are needed for deep-subwavelength focusing. These results provide the required elements of intuition to understand light concentration at the nanometer scale and to design optimized systems for application in ultrasensitive optical analyses and nonlinear photonics.

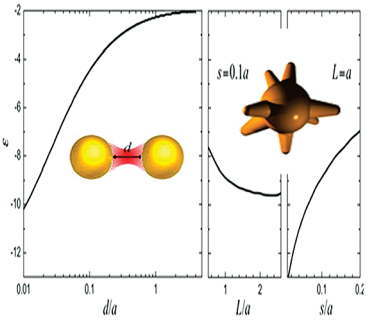

Many of the physical and chemical elementary processes that are relevant for life involve energy exchanges in the electronvolt range. This corresponds to visible and near-infrared optical excitations. The wavelength of light in that energy window is too large to resolve nanometer structures such as biomolecules or cell components. This is a result of the so-called diffraction limit,[1] which states that it is impossible to concentrate optical energy within a region much smaller than the wavelength in a homogeneous medium using freely propagating light waves. Several ingenious methods have been devised to break that limit and push spatial resolution of optical techniques down to truly nanometer scales. For instance, quantum light can increase resolution in proportion to the number of entangled photons;[2] likewise, nonlinear processes can produce an increase in resolution because their probability is proportional to a power of the light intensity;[3] superoscillating functions describing certain arrangements of far-field light can also produce sharp spots,[4,5] but they are surrounded by regions of high light intensity. A different approach consists of exploiting evanescent fields, such as those occurring in the far side of a prism illuminated under total internal reflection (TIR) conditions. By definition, evanescent fields possess components of wave vectors exceeding those of propagating waves, so that they naturally describe fast field variations compared to the wavelength. This property has been used to increase resolution, which can reach faithful imaging in the case of Pendry's perfect lens, although it relies on the existence of nonabsorbing negative-index materials,[6] which are only available at microwave frequencies,[7] a problem that can be partially circumvented by his electrostatic version of the lens, using surface plasmons.[8]

Many of the physical and chemical elementary processes that are relevant for life involve energy exchanges in the electronvolt range, which corresponds to visible and near-infrared optical excitations. The wavelength of light in that energy window is too large to resolve nanometer structures such as biomolecules or cell components.

An important property of evanescent waves is that, unlike conventional propagating waves, they do not transport energy, and therefore, they can produce large amplification of the electric field without violating energy conservation.

Received Date: June 16, 2010
Accepted Date: July 16, 2010
Published on Web Date: July 27, 2010

DOI: 10.1021/jz100820m | *J. Phys. Chem. Lett.* **2010**, *1*, 2428–2434

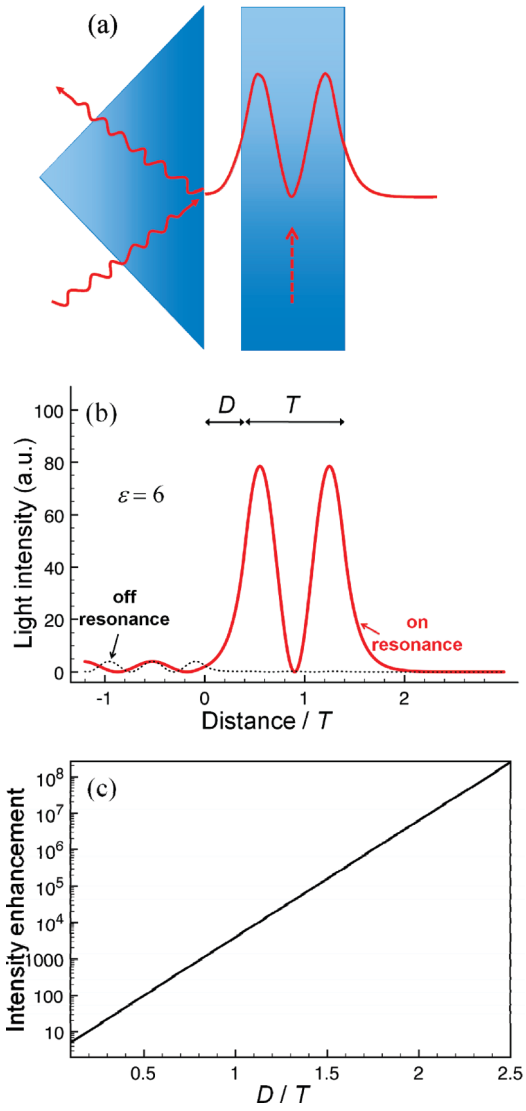

Figure 1. Optical field amplification assisted by coupling to evanescent modes in a planar waveguide. (a) Light spilling out from a prism under total internal reflection can couple to a guided mode in a planar dielectric film. The dashed arrow indicates the direction of propagation of the guided mode along the film. (b) Field amplification for a case where both the prism and the waveguide have a permittivity six times higher than that of the material in the gap and to the right of the waveguide. The light is TE-polarized and incident under 45°. The electric field intensity is given relative to the incident intensity at wavelengths that are on- ($\lambda \approx 2.41T$) and off-resonance ($\lambda = 1.5T$) in the waveguide. Distances are measured relative to the thickness of the waveguide film, T. (c) On-resonance field intensity at the entry side of the waveguide as a function of gap distance D.

A tutorial example of how this can be used for sensing is given in Figure 1. The upper part of this figure shows a prism on the left-hand side illuminated under TIR. The evanescent light spilling out toward the right-hand side of the prism interacts with a dielectric layer waveguide. The light frequency and the angle of incidence, which determine the amount of wave vector parallel to the guide, are tuned to match those for a guided mode of the film. Under these conditions, the intensity is amplified in the gap region via coupling to the evanescent wave component spilling out from the left-hand side of the film, in which it reaches high values. Both the prism and the waveguide materials are assumed to have a positive permittivity six times higher than that of the medium in the gap and to the right of the waveguide. The field intensity along the direction perpendicular to the gap of this structure is shown in more detail in Figure 1b, as obtained from an analytical resolution of Maxwell's equations for the specific geometrical conditions defined in the figure. Obviously, under resonance conditions, the intensity in the film must increase exponentially with gap spacing, and this is what actually comes out from the simulation, as shown in Figure 1c. The material inside of the film (e.g., a liquid layer) is thus exposed to a high light intensity, which can facilitate optical detection through the resulting amplification of light scattering.

A frustrated TIR phenomenon similar to that occurring in Figure 1 has found application to study surface plasmon polaritons, which are also evanescent guided modes in a planar metal surface rather than a dielectric film.[9] The confined nature of surface plasmons emphasizes their evanescent wave character; they decay inside of the metal due to the exclusion of electromagnetic fields in the bulk of these materials and also outside of the metal because they have large wave vectors compared to that of light in the surrounding medium. Actually, plasmons can be used to resolve subwavelength structures, thus breaking the diffraction limit down to arbitrarily small length scales in the electrostatic domain. Additionally, these excitations provide a practical solution to achieve deep-subwavelength optical energy concentration; metallic sharp tips[10] and narrow gaps[11] can host optical hot spots, in which light amplification is only limited by metal absorption and coupling to propagating light. This is used in surface-enhanced Raman scattering (SERS)[12] to increase the Raman signal by over 10 orders of magnitude,[11] thus facilitating the optical identification of single molecules. In a different context, this increase in local field intensity enhances nonlinear scattering,[13] which can be potentially useful for optical signal processing.

The confined nature of surface plasmons emphasizes their evanescent wave character, and they can be used to resolve subwavelength structures, thus breaking the diffraction limit down to arbitrarily small length scales in the electrostatic domain.

Much of the work done on SERS relies on the existence of optical hot spots, although their precise morphology and underlying mechanisms have eluded detailed analysis. Despite the interest triggered by the enormous possibilities of

DOI: 10.1021/jz100820m | J. Phys. Chem. Lett. 2010, 1, 2428–2434

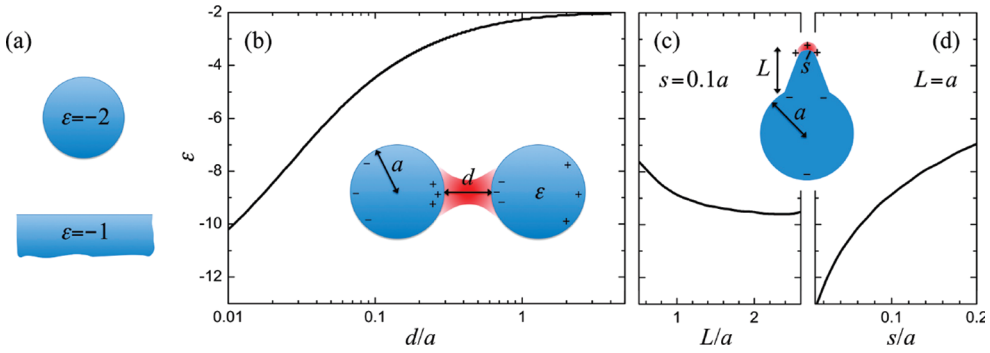

Figure 2. Values of the permittivity ε that are consistent with the existence of localized excitations in various surface morphologies. (a) An isolated sphere and a plane. (b) Sphere dimer, as a function of surface-to-surface separation d, normalized to the radius a. (c, d) Tip protuberance in a sphere, as a function of sphere radius a, tip length L, and rounding radius of the tip apex s. The values of ε are assumed to be real and given relative to the environment, as obtained from the electrostatic limit. The red regions and the ± signs schematically indicate where the field and surface charges are concentrated.

this technique for ultrasensitive bioassays, leading to exotic proposals for extraordinary field amplification such as Stockman's self-similar lens,[14] the production of hot spots has remained largely out of control. This scenario has been improved by the synthesis of new particles exhibiting sharp tips with an apex radius of only a few nanometers,[15] which have been successfully used to produce up to 10 orders of magnitude of SERS enhancement under controlled conditions (see below).[10]

Before discussing further aspects of hospots and their application to SERS, let us briefly turn our attention toward a more fundamental question, why metals are needed to confine electromagentic energy in tiny subwavelength spaces or, equivalently, why negative-permittivity $\varepsilon < 0$ materials are required for that purpose. The relevant distances with which we are concerned are sufficiently small so as to neglect retardation effects, and therefore, we can address this question by examining Poisson's equation. Actually, the minimum particle size compatible with the existence of well-defined hot spots is only limited by broadening due to nonlocal effects (see below). Figure 2a illustrates the required values of ε relative to the dielectric environment that are necessary to achieve localized modes in individual spheres and planar surfaces (i.e., the values required to sustain a resonance). Panels (b−d) of that figure represent ε, both in dimers for the lowest-order dipolar mode as a function of gap distance and in tips as a function of length and apex curvature. We confirm from this plot that metals are indeed required in these cases because all values of ε turn out to be negative. This is easy to explain by relying on physical intuition derived from the formal equivalence between Poisson's equation and the steady-state heat transport equation.[16] The dielectric function ε and the potential ϕ in electrostatics play exactly the same role as the thermal conductivity κ and the temperature T in thermostatics. More precisely, in the absence of external electric or thermal sources, they satisfy the relations $\nabla\cdot\varepsilon\nabla\phi = 0$ and $\nabla\cdot\kappa\nabla T = 0$. Now, the relevant piece of intuition is that we cannot confine heat in a localized region of space using passive materials (i.e., without an external energy supply), and since these materials have positive thermal conductivity, as guaranteed by the second law of thermodynamics (heat does flow toward regions of lower temperature), we conclude from the electrostatic analogy that dielectrics with positive permittivity cannot trap electromagnetic energy.

Narrow gaps and tips cover a wide spectrum of metallic nanostructures that can be synthesized in practice for sensing applications. In a dimer, the isolated particle limit of Figure 2b is asymptotically approached as $\varepsilon = -2-6a^3/(2a+d)^3$, when $d \gg a$. This expression arises from an analytical expansion of the dimer response consisting of a representation of spheres as dipoles. In the near-touching limit, the gap mode permittivity scales as $\varepsilon \approx -(a/d)^{1/2}$, and a singular transition takes place right at touching conditions, with new modes arising when the particles overlap.[17] Charges associated to these modes (± signs in Figure 2b) accumulate near the gap, leading to a huge enhancement of the field. Charge neutrality in each of the particles is ensured by less concentrated charges distributed over a wide region away from the gap. In tips, the most relevant geometrical parameter is the curvature of the apex, which produces dramatic variations in the tip plasmon permittivity, as shown in Figure 2d. In contrast, the dependence on tip length is rather smooth, essentially comprising a smooth decrease in ε with increasing length.

Like most electromagnetic simulations in this context, Figures 1 and 2 were obtained under the assumption of local response, whereby the electric displacement at each point in a material is considered to depend exclusively on the frequency-dependent dielectric function and the electric field at exactly the same point. However, for the short distances under consideration, nonlocal dispersion effects in the dielectric response can be important.[18] This is the case when one studies the interaction among charges (e.g., induced charges) across distances comparable to the Thomas−Fermi screening length of a metal in the electrostatic regime and, more generally, at finite frequency ω, when the distances involved are comparable to the inverse of the so-called Landau damping cutoff wavevector $\sim\omega/v_F$, where v_F is the Fermi velocity.[19] In the local approximation, induced charges are concentrated right at the sharp interfaces separating different materials, whereas nonlocal effects lead to a finite penetration length $\sim\omega/v_F$ of these charges within metals. As a result, the interaction of particles in close proximity turns out to be weaker when nonlocality is taken into account. This effect is

DOI: 10.1021/jz100820m | J. Phys. Chem. Lett. 2010, 1, 2428–2434

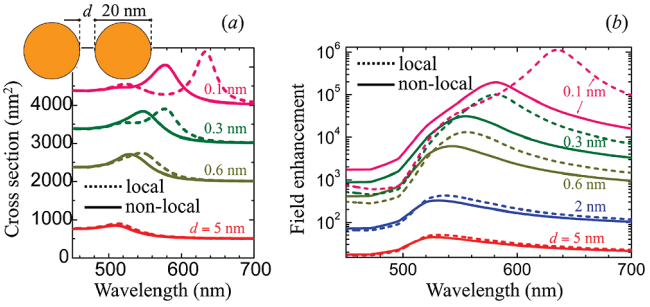

Figure 3. Nonlocal effects in gold dimers. (a) Extinction spectra calculated for gold dimers (see inset) both with (solid curves) and without (dashed curves) consideration of nonlocal effects. The external electric field is directed across the gap. Different gap distances *d* are considered, as labeled. (b) Electric field intensity enhancement at the center of the dimers, under the same conditions as those in (a). Reproduced with permission from ref 18, Copyright 2008, American Chemical Society.

clearly visible as a weakening of the field enhancement in the dimers considered in Figure 3b. Likewise, the plasmon peak positions are shifted toward lower values of $\mathrm{Re}\{-\varepsilon\}$ and, therefore, toward the blue when examining resonances in the near-infrared (Figure 3a). At sufficiently small distances, the finite penetration of the density of conduction electrons outside of the metal can lead to electron tunneling coupling and an increased role of dissipation. This regime has been recently explored through ab initio electronic simulations based upon the time-dependent local density approximation for a jellium representing spherical dimers of subnanometer particles.[20] Further work in this direction needs to be done in order to assess the effect of electronic overlap between neighboring particles of larger size.

We focus in the final part on the application of light concentration toward SERS spectroscopy. SERS was discovered more than 30 years ago,[21] and the theory behind the underlying mechanisms, chemical and electromagnetic, is now mature.[12] Therefore, research is rapidly turning into the design of materials that can yield stable and reproducible SERS intensities, so that we can fully exploit its analytical potential in fields such as biomedicine, environment, or materials characterization. SERS largely relies on localized surface plasmons and, in particular, on the associated high confinement of electromagnetic energy, which particularly occurs within narrow gaps between metal nanoparticles but also at sharp nanoscale corners and edges.[22,23] The enormous intensity enhancement factors associated with localized surface plasmons, up to 5 orders of magnitude,[11] directly translate into an increase of electronic transition probabilities for atoms or molecules exposed to such fields. In particular, SERS by molecules starts with an electronic excitation, followed by inelastic coupling to internal vibrational levels of the molecule and a subsequent radiative decay and emission, thus involving two electronic transitions and therefore undergoing signal enhancement factors up to 10 orders of magnitude by coupling to plasmonic hot spots.[11]

So far, SERS hot spots have been often created by simply exploiting the short-length gaps between nanostructures originating from simple aggregation in colloids, which can be easily promoted by changing the solvent, increasing the ionic strength of the suspension, decreasing solution pH, or just spontaneously due to the adsorption of the analyte. However, this uncontrolled aggregation process is usually undesired because it leads to a random distribution of hot spots, and therefore, the signal varies from particle to particle. Thus, several approaches have been developed for the controlled production of hot spots. In fact, increasing activity is observed in the development of wet chemical methods for the controlled fabrication of SERS-active nanoparticle dimers, including spheres, cages, pyramids, or rods.[24−27] Conversely, fabrication of thin solid films with the ability of yielding highly homogeneous SERS intensity is also being exploited through grating patterning,[28] colloidal stamping,[29] block copolymer micelles,[30] or nanosphere lithography.[31]

The discovery of the concentration of plasmonic fields at sharp tips within anisotropic nanoparticles, such as triangles, nanorods, or nanostars[10,32] paved the way toward the development of a new family of SERS substrates that are capable of concentrating light in specific points of their surface (Figure 4a). Among the different possible anisotropic nanostructures, materials resembling a central structure with radial acute tips branching out, nanostars, have been demonstrated to yield particularly high SERS intensity.[10,27,33−36] However, as discussed above, the optimum configuration for maximum enhancement should also include the presence of a nanoscale gap. By careful design of the appropriate experiment, a single molecule can be attached at the tip of a single nanostar and confined next to a metal surface, which has made possible the first demonstration of single-molecule, single-particle SERS spectroscopy (Figure 4b; the density of SERS-active molecules is made so low in the experiment that it is rather unlikely to have more than one of them under each individual particle).[10] While experimental and theoretical calculations show that nanostars deposited onto a smooth gold thin film produce a SERS enhancement of around 2 orders of magnitude larger than regular hot spots created by controlled dimer assembly (Figure 4c), the presence of the film appears to have a deep impact on the increase of the Raman signal, which has been explained in terms of nonlocal effects and quantum confinement.[18] Experimental evidence for this was also obtained through the simultaneous detection of two analytes (Figure 4d).[27] In this experiment, a monolayer of an aromatic dithiol (1,5-naphthalenedithiol, 15NAT) was self-assembled onto a smooth gold film; gold-thorned nanowires (elongated nanoparticles in which sharp tips were grown from a central gold nanowire) were then deposited with controlled density, and subsequently, a second aromatic thiol (benzenethiol, BT) was assembled from the gas phase. The results showed that, although BT has 10-fold larger SERS cross section than 15NAT, and even considering that the amount of BT retained on the surface was much larger than that of 15NAT, the SERS spectra were dominated by the characteristic bands of 15NAT, which was confined between the tips and the gold film. Still, the SERS-based analytical application of nanostar-like colloids can be foreseen by simply depositing a monolayer of the analyte on a smooth gold surface and spin-coating or -casting the nanostars on top of it, thereby generating a sandwich

DOI: 10.1021/jz100820m | J. Phys. Chem. Lett. 2010, 1, 2428–2434

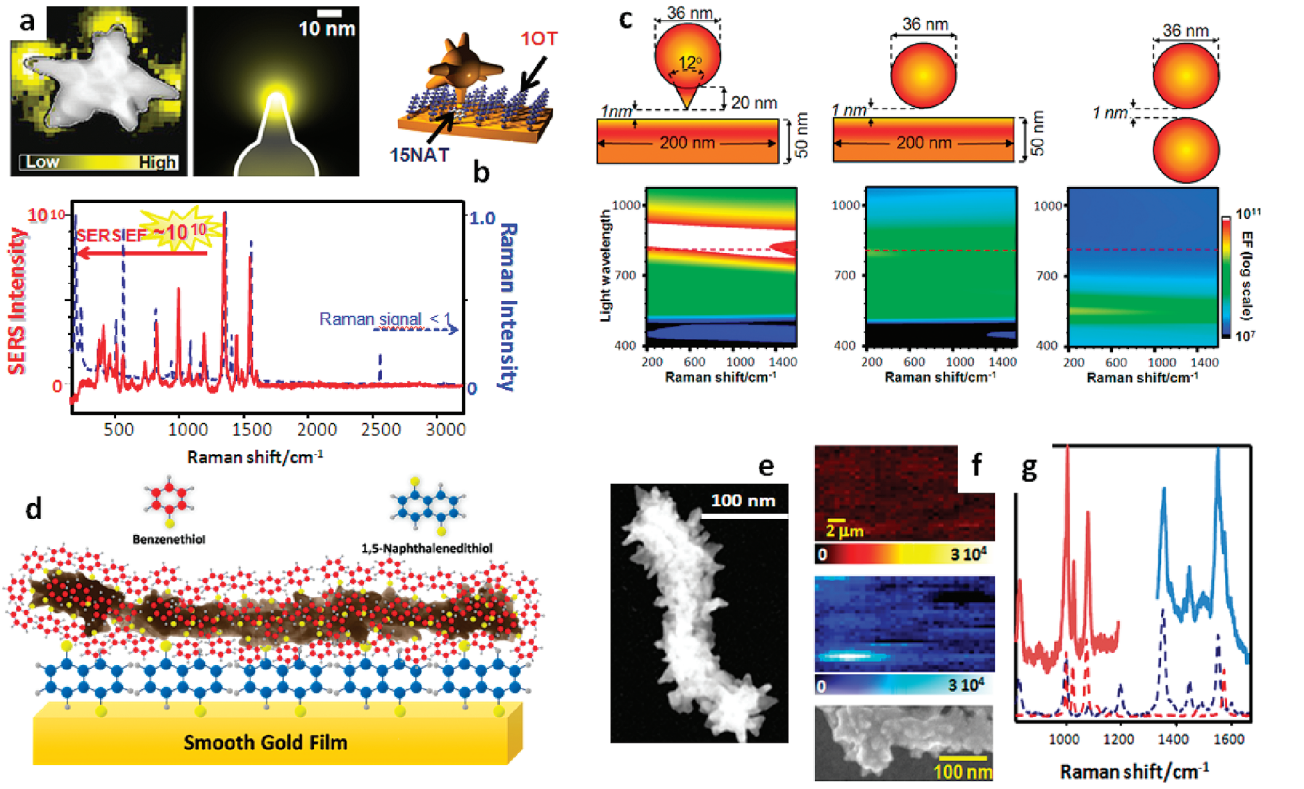

Figure 4. (a) High-resolution STEM dark-field image of an individual Au nanostar overlapped with EELS intensity mapping, and calculated EELS intensity map of the plasmon resonance in a particle with a tip; maximum electron energy loss at the tip apexes confirms light localization at those sites for the tip plasmon energy. (b) Sketch of the deposition of single nanostars onto single molecules through thiol binding exclusively onto 1,5-naphthalenedithiol (15NAT), which is also the optically active analyte, diluted in a 1-octanethiol (1OT, optically inactive) self-assembled monolayer. Experimental bulk Raman spectrum of a concentrated solution of 15NAT and SERS spectrum of the same molecule located in the confined region between the nanostar and gold film, showing an overall enhancement factor larger than 10^{10}. (c) Schematic representation and calculated SERS enhancement factor as a function of the Raman shift and laser wavelength for three different configurations of nanoscale gaps: a sphere with a tip near a gold film, a sphere near a gold film, and a dimer of gold spheres. It is obvious that the tip−film configuration provides maximum enhancement. (d) Schematic representation of the two-analyte method for the evaluation of the SERS efficiency in different regions of a thorned nanowire (TNW) surface. Briefly, TNWs are self-assembled (through the tips) onto an optically active monolayer of 15NAT and in turn deposited on a smooth gold film; then, benzenethiol (BT) is adsorbed over the entire TNW surface from the gas phase. (e) High-resolution SEM image of a thorned nanowire, showing the high density of spikes with sharp tips. (f) SERS mapping of BT (red) and 15NAT (blue) acquired from the same region of the sample and demonstrating uniform intensity for both analytes. (g) Representative spectra for the simultaneous detection of BT and 15NAT. Dashed lines correspond to individual SERS spectra of BT and 15NAT. Reproduced with permission from refs 10 and 27, Copyright 2009 and 2010, American Chemical Society.

between the tips and the surface. This approach has been successfully applied for ultrasensitive detection of phenol.[37]

Experimental and theoretical calculations show that nanostars deposited onto a smooth gold thin film produce a large SERS enhancement. The presence of the film appears to have a deep impact on the increase of the Raman signal.

The advances here discussed provide us with a global understanding of the mechanisms involved in near-field enhancement and its applications to sensing (SERS in particular). From a practical point of view, the question remains, what is the largest possible field enhancement that can be achieved at a nanometer-sized spot. The combination of metallic sharp tips and narrow gaps, such as those found when nanostars are placed near a planar surface, seems to provide a close-to-optimum solution. However, further work needs to be done to improve the sharpness and size distribution of the tips. The choice of material is also important, and in particular, silver is expected to perform better than gold since it is less absorptive, leading to narrower plasmon resonances, but chemical oxidation may become a problem in this case. Larger field enhancement and confinement are thus key ingredients to access individual molecules in the complex environment often encountered when examining biological samples. In the foreseeable future, these techniques could lead to comprehensive molecule-by-molecule analysis of samples down to the zeptomol

DOI: 10.1021/jz100820m | J. Phys. Chem. Lett. 2010, 1, 2428–2434

regime, as needed, for instance, for analyzing, replicating, and modifying genetic material.

The combination of metallic sharp tips and narrow gaps, such as those found when nanostars are placed near a planar surface, seems to provide a close-to-optimum solution for identifying the largest possible field enhancement that can be achieved at a nanometer-sized spot.

An experimental assessment of the importance of nonlocality in the description of the optical response is still missing. However, the experimental uncertainty in the determination of gap distances and exact surface morphology leads to a wide range of absolute values in the reported measured spectra that are sensitive to this parameter (e.g., in SERS and luminescence from molecules sandwiched in narrow metallic gaps). Metallic nanoparticles with narrow-size distribution will have to be produced in order to measure the blue shifts and decrease in field enhancement predicted by theory.

Optics at the nanoscale appears to be a field of increasing activity, with the prospect of truly controlling the quasi-electrostatic near-field and its in/out coupling to external light. Recent efforts in coherent control point in this direction.[38,39] Simultaneously, an extension of the concepts of macroscopic electronics has been proposed to deal with these new systems.[40]

AUTHOR INFORMATION

Corresponding Author:

*To whom correspondence should be addressed. E-mail: J.G.deAbajo@csic.es (F.J.G.A.); lmarzan@uvigo.es (L.M.L.-M.).

Biographies

Ramón A. Alvarez-Puebla is a Research Fellow at the University of Vigo. He worked as a Postdoc at the University of Windsor (Canada) and as a Research Officer at the National Institute for Nanotechnology (NRC). His interests involve electronic and vibrational spectroscopy, surface-enhanced spectroscopy, and their applications in sensing.

Luis M. Liz-Marzán is a Professor at the University of Vigo. He was a Postdoctoral Fellow at Utrecht University and a visiting professor at Tohoku University and the University of Michigan. He is Fellow of the RSC, Senior Editor of Langmuir, and received a Humboldt Research Award, among others.

F. Javier García de Abajo is a Research Professor at the Spanish Scientific Research Council (CSIC). He visited Berkeley National Lab during 1997−2000 and is currently spending a sabbatical year at the University of Southampton. He is Deputy Editor of Optics Express and Fellow of the APS and the OSA.

ACKNOWLEDGMENT This work has been supported by the Spanish MICINN (MAT2007-62696, MAT2007-66050, MAT2008-05755, Consolider NANOBIOMED, and Consolider NanoLight.es) and the EU (Grants CP-248236- INGENIOUS and NMP4-SL-2008-213669-ENSEMBLE).

REFERENCES

(1) Abbe, E. Beiträge zur Theorie des Mikroskops und der Mikroskopischen Wahrnehmungen. *Arch. Mikrosk. Anat. Entwicklungsmech.* **1873,** *9*, 413–468.

(2) Boto, A. N.; Kok, P.; Abrams, D. S.; Braunstein, S. L.; Williams, C. P.; Dowling, J. P. Quantum Interferometric Optical Lithography: Exploiting Entanglement to Beat the Diffraction Limit. *Phys. Rev. Lett.* **2000,** *85*, 2733–2736.

(3) Cumpston, B. H.; Ananthavel, S. P.; Barlow, S.; Dyer, D. L.; Ehrlich, J. E.; Erskine, L. L.; Heikal, A. A.; Kuebler, S. M.; Lee, I. Y. S.; McCord-Maughon, D.; et al. Two-Photon Polymerization Initiators for Three-dimensional Optical Data Storage and Microfabrication. *Nature* **1999,** *398*, 51–54.

(4) Berry, M. V.; Popescu, S. Evolution of Quantum Superoscillations and Optical Superresolution without Evanescent Waves. *J. Phys. A* **2006,** *39*, 6965–6977.

(5) Huang, F. M.; Chen, Y.; García de Abajo, F. J.; Zheludev, N. I. Optical Super-resolution Through Super-oscillations. *J. Opt. A: Pure Appl. Opt.* **2007,** *9*, S285–S288.

(6) Pendry, J. B. Negative Refraction Makes a Perfect Lens. *Phys. Rev. Lett.* **2000,** *85*, 3966–3969.

(7) Smith, D. R.; Pendry, J. B.; Wiltshire, M. C. K. Metamaterials and Negative Refractive Index. *Science* **2004,** *305*, 788–792.

(8) Fang, N.; Lee, H.; Sun, C.; Zhang, X. Sub-Diffraction-Limited Optical Imaging with a Silver Superlens. *Science* **2005,** *308*, 534–537.

(9) Raether, H. *Surface Plasmons on Smooth and Rough Surfaces and on Gratings*; Springer-Verlag: Berlin, Germany, 1988; Vol. 111.

(10) Rodríguez-Lorenzo, L.; Alvarez-Puebla, R. A.; Pastoriza-Santos, I.; Mazzucco, S.; Stéphan, O.; Kociak, M.; Liz-Marzán, L. M.; García de Abajo, F. J. Zeptomol Detection Through Controlled Ultrasensitive Surface-Enhanced Raman Scattering. *J. Am. Chem. Soc.* **2009,** *131*, 4616–4618.

(11) Xu, H.; Bjerneld, E. J.; Käll, M.; Borjesson, L. Spectroscopy of Single Hemoglobin Molecules by Surface Enhanced Raman Scattering. *Phys. Rev. Lett.* **1999,** *83*, 4357–4360.

(12) Moskovits, M. Surface-Enhanced Raman Spectroscopy: A Brief Retrospective. *J. Raman Spectrosc.* **2005,** *36*, 485–496.

(13) Danckwerts, M.; Novotny, L. Optical Frequency Mixing at Coupled Gold Nanoparticles. *Phys. Rev. Lett.* **2007,** *98*, 026104/1–026104/4.

(14) Li, K. R.; Stockman, M. I.; Bergman, D. J. Self-Similar Chain of Metal Nanospheres as an Efficient Nanolens. *Phys. Rev. Lett.* **2003,** *91*, 227402/1–227402/4.

(15) Kumar, P. S.; Pastoriza-Santos, I.; Rodríguez-González, B.; García de Abajo, F. J.; Liz-Marzán, L. M. High-Yield Synthesis and Optical Response of Gold Nanostars. *Nanotechnol.* **2008,** *19*, 015606/1–015606/5.

(16) Baffou, G.; Quidant, R.; García de Abajo, F. J. Nanoscale Control of Optical Heating in Complex Plasmonic Systems. *ACS Nano* **2010,** *4*, 709–716.

(17) Romero, I.; Aizpurua, J.; Bryant, G. W.; García de Abajo, F. J. Plasmons in Nearly Touching Metallic Nanoparticles: Singular Response in the Limit of Touching Dimers. *Opt. Express* **2006,** *14*, 9988–9999.

(18) García de Abajo, F. J. Nonlocal Effects in the Plasmons of Strongly Interacting Nanoparticles, Dimers, and Waveguides. *J. Phys. Chem. C* **2008,** *112*, 17983–17987.

(19) Larkin, I. A.; Stockman, M. I. Imperfect Perfect Lens. *Nano Lett.* **2005,** *5*, 339–343.
(20) Zuloaga, J.; Prodan, E.; Nordlander, P. Quantum Description of the Plasmon Resonances of a Nanoparticle Dimer. *Nano Lett.* **2009,** *9*, 887–891.
(21) Fleischmann, M.; Hendra, P. J.; McQuillan, A. J. Raman Spectra of Pyridine Adsorbed at a Silver Electrode. *Chem. Phys. Lett.* **1974,** *26*, 163–166.
(22) Hao, E.; Bailey, R.; Schatz, G.; Hupp, J. T.; Li, S. Synthesis and Optical Properties of "Branched" Gold Nanocrystals. *Nano Lett.* **2004,** *4*, 327–330.
(23) Prodan, E.; Radloff, C.; Halas, N. J.; Nordlander, P. A Hybridization Model for the Plasmon Response of Complex Nanostructures. *Science* **2003,** *302*, 419–422.
(24) Stoerzinger, K. A.; Hasan, W.; Lin, J. Y.; Robles, A.; Odom, T. W. Screening Nanopyramid Assemblies to Optimize Surface Enhanced Raman Scattering. *J. Phys. Chem. Lett.* **2010,** *1*, 1046–1050.
(25) Cobley, C. M.; Rycenga, M.; Zhou, F.; Li, Z. Y.; Xia, Y. Etching and Growth: An Intertwined Pathway to Silver Nanocrystals with Exotic Shapes. *Angew. Chem., Int. Ed.* **2009,** *48*, 4824–4827.
(26) Braun, G. B.; Lee, S. J.; Laurence, T.; Fera, N.; Fabris, L.; Bazan, G. C.; Moskovits, M.; Reich, N. O. Generalized Approach to SERS-Active Nanomaterials via Controlled Nanoparticle Linking, Polymer Encapsulation, and Small-Molecule Infusion. *J. Phys. Chem. C* **2009,** *113*, 13622–13629.
(27) Pazos-Pérez, N.; Barbosa, S.; Rodríguez-Lorenzo, L.; Aldeanueva-Potel, P.; Pérez-Juste, J.; Pastoriza-Santos, I.; Alvarez-Puebla, R. A.; Liz-Marzán, L. M. Growth of Sharp Tips on Gold Nanowires Leads to Increased Surface-Enhanced Raman Scattering Activity. *J. Phys. Chem. Lett.* **2010,** *1*, 24–27.
(28) Deng, X.; Braun, G. B.; Liu, S.; Sciortino, P. F., Jr.; Koefer, B.; Tombler, T.; Moskovits, M. Single-Order, Subwavelength Resonant Nanograting as a Uniformly Hot Substrate for Surface-Enhanced Raman Spectroscopy. *Nano Lett.* **2010,** *10*, 1780–1786.
(29) Pazos-Pérez, N.; Ni, W.; Schweikart, A.; Alvarez-Puebla, R. A.; Fery, A.; Liz-Marzán, L. M. Highly Uniform SERS Substrates Formed by Wrinkle-confined Drying of Gold Colloids. *Chem. Sci.* **2010,** *1*, 174−178.
(30) Sánchez-Iglesias, A.; Aldeanueva-Potel, P.; Ni, W.; Pérez-Juste, J.; Pastoriza-Santos, I.; Alvarez-Puebla, R. A.; Mbenkum, B. N.; Liz-Marzán, L. M. Chemical Seeded Growth of Ag Nanoparticle Arrays and their Application as Reproducible SERS Substrates. *Nano Today* **2010,** *5*, 21–27.
(31) Camden, J. P.; Dieringer, J. A.; Zhao, J.; Van Duyne, R. P. Controlled Plasmonic Nanostructures for Surface-Enhanced Spectroscopy and Sensing. *Acc. Chem. Res.* **2008,** *41*, 1653–1661.
(32) Nelayah, J.; Kociak, M.; Stéphan, O.; García de Abajo, F. J.; Tencé, M.; Henrard, L.; Taverna, D.; Pastoriza-Santos, I.; Liz-Marzán, L. M.; Colliex, C. Mapping Surface Plasmons on a Single Metallic Nanoparticle. *Nat. Phys.* **2007,** *3*, 348–353.
(33) Hrelescu, C.; Sau, T. K.; Rogach, A. L.; Jackel, F.; Feldmann, J. Single Gold Nanostars Enhance Raman Scattering. *App. Phys. Lett.* **2009,** *94*, 153113.
(34) Khoury, C. G.; Vo-Dinh, T. Gold Nanostars For Surface-Enhanced Raman Scattering: Synthesis, Characterization and Optimization. *J. Phys. Chem. C* **2008,** *112*, 18849–18859.
(35) Hao, F.; Nehl, C. L.; Hafner, J. H.; Nordlander, P. Plasmon Resonances of a Gold Nanostar. *Nano Lett.* **2007,** *7*, 729–732.
(36) Nehl, C. L.; Liao, H.; Hafner, J. H. Optical Properties of Star-Shaped Gold Nanoparticles. *Nano Lett.* **2006,** *6*, 683–688.
(37) Rodríguez-Lorenzo, L.; Álvarez-Puebla, R. A.; Garcia de Abajo, F. J.; Liz-Marzán, L. M. Surface Enhanced Raman Scattering Using Star-Shaped Gold Colloidal Nanoparticles. *J. Phys. Chem. C* **2010,** *114*, 7336–7340.
(38) Aeschlimann, M.; Bauer, M.; Bayer, D.; Brixner, T.; Garcia de Abajo, F. J.; Pfeiffer, W.; Rohmer, M.; Spindler, C.; Steeb, F. Adaptive Subwavelength Control of Nano-optical Fields. *Nature* **2007,** *446*, 301–304.
(39) Utikal, T.; Stockman, M. I.; Heberle, A. P.; Lippitz, M.; Giessen, H. All-Optical Control of the Ultrafast Dynamics of a Hybrid Plasmonic System. *Phys. Rev. Lett.* **2010,** *104*, 113903/1–113903/4.
(40) Engheta, N. Circuits with Light at Nanoscales: Optical Nanocircuits Inspired by Metamaterials. *Science* **2007,** *317*, 1698–1702.

DOI: 10.1021/jz100820m | *J. Phys. Chem. Lett.* **2010,** *1*, 2428–2434